Monthly Notices of the ROYAL ASTRONOMICAL SOCIETY

MNRAS **527,** 12268–12283 (2024) https://doi.org/10.1093/mnras/stad3994
Advance Access publication 2024 January 8

Properties of the gas escaping from a non-isothermal porous dust surface layer of a comet

Yu. Skorov,[1,2]★ V. Reshetnyk,[3,4] J. Markkanen,[2] S. Mottola,[5] W. Macher,[6] O. Mokhtari,[7] N. Thomas,[7] M. Küppers[8] and P. Hartogh[1]

[1]*Max – Planck – Institut für Sonnensystemforschung, Justus – von – Liebig – Weg 3, D-37077 Göttingen, Germany*
[2]*Institut für Geophysik und extraterrestrische Physik, Technische Universität Braunschweig, Mendelssohnstr. 3, D-38106 Braunschweig, Germany*
[3]*Taras Shevchenko National University of Kyiv, Glushkova ave. 2, 01601 Kyiv, Ukraine*
[4]*Main Astronomical Observatory of National Academy of Science of Ukraine, Akademika Zabolotnoho Str. 27, 03680 Kyiv, Ukraine*
[5]*DLR Institute of Planetary Research, Rutherfordstrasse, 2, D-12489 Berlin, Germany*
[6]*Space Research Institute, Austrian Academy of Sciences, Schmiedlstrasse 6, A-8042 Graz, Austria*
[7]*Physikalisches Institut, University of Bern, Bern, Sidlerstrasse 5, CH-3011, Switzerland*
[8]*European Space Agency (ESA), ESAC, Camino Bajo del Castillo s/n, E-28692 Villanueva de la Cañada, Madrid, Spain*

Accepted 2023 December 15. Received 2023 December 14; in original form 2023 October 5

ABSTRACT

Estimation of the properties of the sublimation products leaving the cometary nucleus is one of the significant questions in the study of the dusty-gas flow following the Rosetta mission. It is widely assumed that the temperature of the water molecules emitted is the temperature of ice directly exposed to the surface. However, it is the simplest non-verified idealization if the refractory porous material lays on the surface and controls the energy driving the ice sublimation. This highly non-isothermal surface layer should change the vapour temperature as the molecules pass through it from the icy region to the vacuum. A key sustaining observation here comes from the MIRO experiment on Rosetta which measured the velocity of water vapour. The observed gas velocities are visibly higher than can be explained by emission at typical ice surface temperature. To investigate the issue, we simulate a gas flow through a non-isothermal porous dust layer and analyse the temperature of molecules emitted. Monodisperse and bimodal layers, as well as layers made of porous aggregates, are considered. Modelling is carried out for various porosity values, different particle sizes, and dust layer thicknesses. The simulation results are embedded in two-layer thermal models including the effective thermal conductivity, volumetric light absorption, and the resistance of the dust layer to the gas flow.

Key words: methods: numerical – comets: general – comets: individual: 67P/Churyumov-Gerasimenko.

1 INTRODUCTION

The discovery of a dust layer covering the surface of the nucleus is arguably one of the main discoveries made by space missions to comets. This was first shown by the instruments on board Giotto's spacecraft (Keller et al. 1986, 1987; Thomas & Keller 1989). From Whipple's concept of a dirty snowball (Whipple 1950), we moved on to a model of an icy dust ball. The following missions to comets made this concept universal and fundamental for the physics of comets. It is the properties of this surface porous layer consisting of non-volatile components of the cometary nucleus that determine the absorption of solar energy and its distribution inside the active near-surface region. And this, in turn, determines the unique activity of comets, concerning both gas and dust.

Theoretical estimates of gas activity are always based on certain thermophysical models allowing the calculation of the rate of sublimation of ice lying under the shielding porous dust layer. We now know a lot about the physical properties of this medium. The reader can find recent reviews in Thomas (2021) and Thomas et al. (2021). For the purposes of this study, it is important to mention that this layer has an extremely low albedo, low thermal inertia, and high porosity (Schloerb et al. 2015; Preusker et al. 2017; Groussin et al. 2019). These properties straightaway make this layer generally highly non-isothermal, i.e. the temperature difference on the scale of a layer thickness can be on the order of a hundred degrees when a comet is in the inner part of the Solar system. Such an inhomogeneity of the temperature field should obviously affect the characteristics of the gas flow during the diffusion of sublimation products into the coma. However, although numerous publications (e.g. Keller et al. 2015b, Blum et al. 2017, Hu et al. 2017, Skorov et al. 2020) are devoted to estimates of the sublimation rate (or, which is the same from the point of view of coma modelling to the estimation of the mass flux), the estimation of the velocity distribution function of the escaping molecules has so far remained in the shadows. In the best case, it was assumed that the effective temperature of the outflowing gas is equal to a weighted average between the temperatures at the surface and at the sublimation front (Keller et al. 2015a; Mottola et al.

★ E-mail: skorov@gmail.com

2020). More often, it was simply assumed that the temperature of the gas is equal to the temperature of the ice exposed on the surface (Marschall et al. 2016). In the last case, the gas temperature was estimated from one simple equation expressing the energy balance on the surface (hereafter we call such an approximation '*Model A*' as introduced by Keller et al. 2015a).

An analysis of Microwave Instrument for the Rosetta Orbiter (MIRO) data showed that such a simplification does not agree well with the results of observations, and therefore the estimation of gas properties on the surface of a cometary nucleus is an urgent practical problem (Marschall et al. 2019; Pinzón-Rodríguez et al. 2021; Rezac et al. 2021). In this work, we use the set of model layers including homogeneous layers of monomers and porous aggregates, as well as heterogeneous layers with cavities and rectangular slits, which are the idealized presentations of real micro-cracks (Skorov et al. 2021, 2022). The range of porosity of the model layers overlaps the estimated range of observational porosity values with a margin. The modelled layers are briefly introduced in the next section.

Using the test particle Monte Carlo (TPMC) method (e.g. Skorov et al. 2011), we study free molecular gas flow (the so-called Knudsen flow) within a random porous medium in the third section. All the results of statistical modelling are performed for a large ensemble of test particles. The sample size is sufficient to obtain an accuracy of about a few per cent for the macroscopic characteristics of escaping particles. We start the analysis with the study of the permeability of the various layers. It is the permeability that makes it possible to estimate the resulting gas production or mass flow. This characteristic, together with other structural layer parameters determines also the energy loss due to ice sublimation. Thus, this analysis is important for the subsequent thermal models. On the assumption that the collision of molecules with dust particles is of a diffusion nature with complete thermal accommodation, the point of the last collision (depth from the surface) uniquely determines the temperature of the emitted molecule if the dust layer temperature is known. We can also evaluate the angular distribution of the velocities of these molecules which is of interest since this distribution may differ from a Maxwell transmission distribution of velocities (Skorov & Rickman 1995).

To estimate the temperature of the escaping gas, it is necessary to know its distribution over the layer. This distribution can be found by solving the heat equation and depends on the energy transfer mechanisms discussed in the fourth section. For layers containing fluffy aggregates or big grains, the radiative thermal conductivity should be taken into account when estimating the effective thermal conductivity. The role of radiative conductivity increases rapidly with growing particle size because it is roughly proportional to the void size between grains. So, we have shown (Skorov et al. 2023b) that for water ice the radiative conductivity plays a major role for aggregates larger than hundreds of microns at all heliocentric distances where water sublimation is significant (up to 3 au). We also consider a volumetric absorption of sunlight in a surface porous layer. This effect (the so-called solid-state greenhouse effect) was modelled by Davidsson & Skorov (2004) and experimentally confirmed by Kaufmann, Kömle & Kargl (2006). For this study, its role is essential because it not only changes the amount of energy supplied to the subliming ice but also changes the temperature distribution in the uppermost part of the layers. This change is directly related to the problem under consideration since the expected region of absorption of solar energy and the region of emission of molecules are located near the upper boundary of the dust layer and have a comparable size. The attenuation of radiation is computed based on geometric optics and the theory of radiative transfer (RT) in a dense medium (Tsang et al. 2007).

In the fifth section, we present the results of modelling the effective temperature of the released gas depending on the basic characteristics of the layer (its thickness and porosity). To this end, two-layer thermal models are used taking into account the relations of the energy balance at the boundaries of the dust layer. We present the results obtained for the two-layer model in the quasi-stationary approximation (named *Model B* following Keller et al. 2015b) and for the two-layer model where the volume absorption of light is considered (this model is based on the Finite Element Method following Skorov et al. 2017). For *Model B*, a comparison is made with the results of *Model A* where the surface temperature is determined from the instantaneous energy balance on the surface (Keller et al. 2015b; 2017). Based on the results obtained, we present illustrative maps, for the gas temperature above the nucleus surface, taking into account the illumination for the realistic shape model of comet 67P (SHAP7 model from Preusker et al. 2017) decimated to about 12 500 triangular facets. The effects of re-radiation and shading were considered. Finally, we discuss which observations are of greatest interest in terms of sensitivity to the role of a hot non-isothermal dust surface layer.

2 LAYER TYPES AND TRANSFER MODEL

Hereafter, we use the model layers that are described in detail in Skorov et al. (2021, 2022). To avoid repetition, below we provide a brief summary of the necessary information, referring the reader to the cited articles for details. For model porous media, various types of elementary construction units and various generation methods are used. In the cases discussed below, the layer is characterized by the filling factor ψ (the ratio of the volume occupied by particles V_s to the total volume of the sample V_m) or porosity ϕ (the difference between the total volume and the volume of particles divided by the total volume of the sample $(V_m - V_s)/V_m = 1 - \psi$). There are no closed pores in our model layers, that is, the pore space is a simply connected volume. The porosity of all considered model layers varied over a wide range, from about 30 per cent to about 90 per cent, i.e. the filling factor changes by more than a factor of 7. We use either solid spherical monomers or porous aggregates as primary units.

The first class of model layers consists of solid spherical monomers. By the different methods of agglomeration, monodisperse or bidisperse layers are created with a random homogeneous or inhomogeneous structure. Random Ballistic Deposition, where a particle sticks at the first point of contact, Random Gravitational Deposition, where the particles roll after the first contact, and Random Sequential Packing, where spheres are placed one by one at random locations within a control volume, are used. In all cases, the primary spheres do not overlap. Model structure inhomogeneities are of two types: rectangular slits or cavities. Slits are considered an idealized analogue of real observed micro-cracks. To generate them, part of the monomers is just removed from the original homogeneous layer to achieve the required effective porosity. Internal cavities are modelled by removing large particles from bidisperse model layers. The characteristic sizes of both slits and cavities usually noticeably exceed the size of the base monomers.

The second large class of layers is the so-called layer with a hierarchical structure. In this case, porous aggregates serve as the basic elements of the layer (elementary units). Observations show that cometary dust particles are more like complex inhomogeneous aggregates (see for example Langevin et al. 2016). To build such model layers having a structure more consistent with observations, a two-step scheme is proposed. In the first stage, the units consisting of solid spheres are created. In our studies, we used dense porous

ensembles of spheres sticking together by ballistic aggregation (BA) with monomer migration after a collision. This method is described in detail in (Shen, Draine & Johnson 2008) and has been successfully used by us to study the optical (Skorov, Keller & Rodin 2008, 2010) and dynamical (Skorov et al. 2016, 2018); properties of cometary dust particles. In the second step of modelling, we use these aggregates to create a random porous medium with a hierarchical structure. An expected nucleus porosity estimated from the observations does not exceed 85 per cent (Preusker et al. 2017). For the model layers, this gives an important constraint on the proper structure of aggregates. The effective porosity of a hierarchical layer can be written as $(1 - \psi_s\psi_A)$, where ψ_s and ψ_A are the volume-filling factors for a layer and an aggregate, respectively. To obtain acceptable values of effective porosity, it is necessary to have aggregates with a volume-filling factor of approximately 40 per cent. This density is possessed by the densest particles considered by Shen, Draine & Johnson (2008). These aggregates are obtained if, after colliding with the target cluster, the monomer can migrate, finding a more 'stable' position. Hereafter, we build on the results of the cited paper and use the aggregates (BAM2) of various sizes constructed there. The required data can be downloaded from the website http://www.astro.princeton.edu/draine/agglom.html.

With the densest aggregates of the BAM2 type taken as model primitives, we turn to build hierarchical layers using two different approaches. In the first case, the model layer was constructed with the YADE computer package (https://www.yade-dem.org), using the discrete element method to simulate the motion of many particles under the action of various physical forces, including the interparticle forces and the external forces (e.g. gravity). In this case, we control all contacts between units during the precipitation and get a necessarily bound skeleton of spheres. In the second approach, called the *method without contact control*, we use an idea proposed for studying the optical and dynamical properties of hierarchical porous aggregates. With this method, the model layer is composed of non-intersecting spherical pseudo-monomers, each of which is a ballistic aggregate of the BAM2 type. When this approach is implemented, the aggregates generally have no contact with each other. This method allows one to study slightly more sparse layers and requires much less computer time for layer generation. A detailed analysis and comparison of these approaches were made in (Skorov et al. 2022).

Based on the methods described, a model cuboid with a side length of several tens of diameters of monomers was constructed.

The diffusion of test particles (for a free molecular gas flow and radiation in the geometrical optics approximation) was simulated using the TPMC method. Its detailed description can be found for example in (Skorov et al. 2021). The synopsis is as follows: In the first step, the centre coordinates of all spheres are loaded into the computer memory. After determining the computation domain, we proceed to model the motion of the test particle. The motion starts at the layer bottom. The coordinates of the entry point are randomly assigned and random values for the velocity are generated following the assumed semi-Maxwellian velocity distribution function in the case of a gas flow. To simulate the attenuation of the intensity of direct solar radiation, it is assumed that all test particles initially move along the inner normal to the lower facet of the cuboid. In the next step, we determine the coordinates of the collision point and new values of the direction cosines are generated on the assumption of diffuse or specular scattering. Then, the next collision point is searched. This procedure is reiterated until the test particle crosses one of the faces of the computational domain. For particles crossing side faces, periodic boundary conditions are used. If the test particle crosses the horizontal faces, the counters of the emitted or absorbed particles change their value, and we proceed to the next test particle. This simulation continues until the counter of particles emitted through the upper face reaches the specified value (usually not smaller than 10 000 particles).

3 TRANSPORT CHARACTERISTICS

3.1 Permeability and mean free path

Our analysis is started by considering a porous layer with permeability Π. In the case of free-molecular (Knudsen) diffusion, permeability can be defined as the ratio of the number of molecules passing the layer to the number of incoming molecules. Even for the simplest model where porosity and layer thickness are fixed, the quantification of permeability depends on the model layer structure (e.g. the model of a bundle of cylindrical capillaries, the model of randomly packed grains, and so on) and the model of molecule scattering (e.g. diffuse or specular). In cometary physics, the capillary model dating back to the work of Knudsen (Knudsen 1909) has widely been used, but less often it was used in the form of the Clausing modification (Clausing 1932). When using both the Knudsen formula and the Clausing formula, permeability is directly proportional to medium porosity and inversely proportional to the so-called tortuosity (see e.g. the discussion in Skorov et al. 2011). In cometary publications, generally, the fixed radius of the capillary tube was considered equal to or proportional to the particle size in the layer. Skorov et al. (2011) presented the dense random packed layer model and showed the constraints of the Knudsen and Clausing models. In particular, it was demonstrated that the relationship between permeability and porosity is non-linear, and the model capillary radius is not equal or proportional to the particle size. However, the capillary model is simple and can be used with due care. We will return to it when analysing the distribution of the last collision of particles. Later, this analysis of random porous media was extended in (Skorov et al. 2021, 2022; Reshetnyk et al. 2021, 2022). In all these studies, we pursued the goal of obtaining, if possible, a satisfactory approximation function of statistic permeability. Such a function would relate the basic layer characteristics (particle size, thickness, and porosity) to permeability so that the latter can be used in thermophysical models to calculate effective gas production.

The scheme of modelling in the cited studies was general. We first calculated the free path-length distribution function (i.e. the distribution of the length of chords between successive scattering events of a test particle by the dust skeleton) and its mean value MFP (Mean Free Path). Then, we obtained the relationship between this mean value and the layer porosity and finally approximated the permeability as a function of the dimensionless thickness expressed via the MFP. Examples of the permeability of some layers are given in Fig. 1. We present cases of uniform layers of spherical monomers and of aggregates of various sizes (the number of monomers in the aggregate is 128 or 512). The results for inhomogeneous layers with slits and models with different scattering (diffuse and specular) are also shown. Note that, accurate modelling of gas-surface interaction is very complicated due to a lack of complete knowledge of surface properties (i.e. of accurate surface interaction potentials). Fully accommodated diffuse reflections are usually assumed for microscopically rough surfaces and low-speed flow at common temperatures. Specular reflection may happen, for example, for a locally smooth surface and when the ratio of masses of the gas molecules to that of the surface molecules is significantly smaller than unity. It is quite common in the kinetic theory of gases to use a simplified microscopic gas–solid interaction model originally

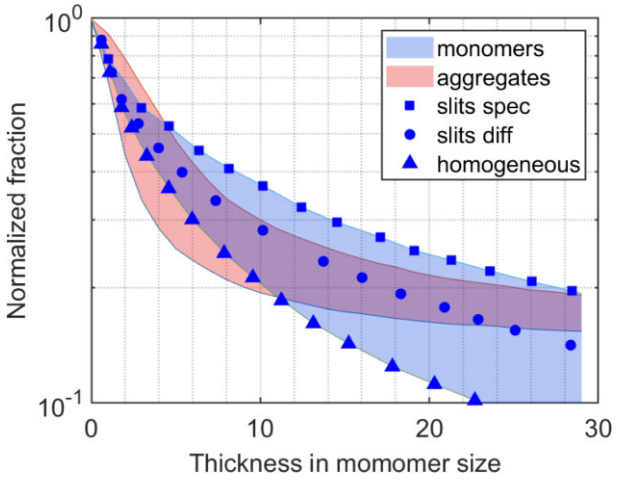

Figure 1. As an illustration, the permeability of different layers is shown as a function of dimensionless thickness. The shaded areas show possible permeability variations for layers of aggregates (due to changes in aggregate size) and for layers of monomers. In the latter case, variations can be caused by inhomogeneities in the layer (slits) as well as by the type of scattering (diffuse or specular). See text for details.

suggested by Maxwell (Maxwell 1879; Bird 1976) which uses only one accommodation coefficient to represent the fractions of diffuse and specular reflections (so-called tangential momentum accommodation coefficient). In the following, diffuse reflection is implied unless otherwise stated.

All illustrative data are collected in one plot to show how variable the permeability is for a layer of a given thickness and approximately the same effective porosity (about 85 per cent) and, hence, how important the microstructure of its structure is. As expected, the lowest permeability has a homogeneous layer of monomers. Both layers with slots and layers of aggregates have greater permeability, which is obviously due to the appearance of 'distant chords' that arise either inside a slit or between bigger porous aggregates. Note that the use of specular scattering significantly increases the permeability in the model with slits, which is associated with the 'heredity' of the initial distribution of the velocity vector of incident molecules. Approximation formulas for the permeability of different layers can be found in the tables presented in the cited papers.

In addition to the obtained approximations of numerical simulations, the theoretical results presented in Macher et al. (2023) can be used. The authors gave the relationship between the permeability of a homogeneous random porous layer and the Knudsen diffusion coefficient of the medium in the free molecular flow regime. In this study, a theoretical probability model was considered, assuming that (i) the medium is homogeneous on a scale larger than the pore size, (ii) the scattering is isotropic and diffuse, and (iii) the bi-hemispherical Maxwell distribution can be applied to the gas molecule velocities following former work by (Asaeda, Yoneda & Toei 1974). For the passage probability, a formula was obtained having the same form as the formula for permeability used for the approximating numerical models in our previous studies, namely

$$\Pi = \frac{1}{1 + L/L_{\rm h}}, \tag{1}$$

where L is the layer thickness and $L_{\rm h}$ distance for which half the gas molecules incident on a model cuboid passes the layer through the pores.

Applying the suggested theoretical approach to the packing of spheres, and based on the results of (Derjaguin 1946) the relation between the mean chord length of the gas molecules (that is equivalent to the above MFP) and the Knudsen gas diffusion coefficient $D^{\rm K}$ was obtained. Based on Fick's law for Knudsen diffusion and the model assumption about Maxwellian velocity distribution of the molecules the formula for $L_{\rm h}$ was derived

$$L_{\rm h} = \frac{4D^{\rm K}}{\phi v_{\rm th}(T)}, \tag{2}$$

where $v_{\rm th} = \sqrt{\frac{8k_{\rm B}T}{\pi m_{\rm g}}}$ is the mean thermal velocity and T is the temperature of the gas, $k_{\rm B}$ is the Boltzmann constant, and $m_{\rm g}$ is the mass of gas molecules.

Derjaguin (1946) considered a dense packed layer of monodisperse spheres of size $d_{\rm s}$ and got the expression for the diffusion coefficient in analogy to Brownian motion via the average square of the displacement of molecules with time, which is a function of the first $\bar{\lambda}$ and second $\overline{\lambda^2}$ moments of the chord length distribution, provided diffuse or specular scattering. Under some simplified assumptions about the chord length distribution, one can write for the monomers of size $d_{\rm d}$

$$\bar{\lambda} \equiv {\rm MFP} = \frac{2\phi}{3(1-\phi)} d_{\rm d}, \qquad \overline{\lambda^2} = 2\bar{\lambda}^2, \tag{3}$$

and finally, for the Knudsen diffusion coefficient

$$D^{\rm K} = \frac{3}{13}\phi\bar{\lambda}v_{\rm th}(T) = \frac{\phi^2}{3\Psi(1-\phi)} v_{\rm th}(T) d_{\rm d}, \tag{4}$$

with $\Psi = 13/6$.

Substituting the resulting expression for $D^{\rm K}$ into the formula (2) for $L_{\rm h}$, we obtain the expression for the permeability

$$\Pi = \frac{1}{1 + \frac{13}{12} L/\bar{\lambda}}, \tag{5}$$

The resulting formula is in good agreement with the approximations that were obtained in numerical models for homogeneous layers. This, in turn, is because the results of numerical simulation of MFP carried out for layers of solid spheres and porous aggregates are in good agreement with the above theoretical estimate of $\bar{\lambda}$. A comparison of theoretical and numerical results is shown in Fig. 2: top panel for the hierarchical layers, and bottom panel for the layers of spherical monomers. The obtained good agreement and relations make it easy to include the attenuation of the gas flow in the thermal model to calculate the resulting gas production. This will be done in the next sections.

3.2 Depth of the last scattering

The permeability analysis presented above quantifies the density of the escaping gas if the sublimation rate is determined. In the next step, we turn to estimating the velocity distribution function of the emitted molecules. In the simplest case of diffuse scattering with complete thermal accommodation, to find the temperature of gas molecules it suffices to analyse the distribution of depths at which the last scattering took place. This function fully determines the kinetic distribution of the absolute value of the velocity for escaping molecules and, hence, the temperature for the released gas. For the first time, the effect of gas heating within the highly non-isothermal cometary surface layer was noted by Skorov & Rickman (1995) and later was applied by Mottola et al. (2020). In the first paper, a model of straight cylindrical capillaries was considered to evaluate the absolute value of the gas velocity and the angular

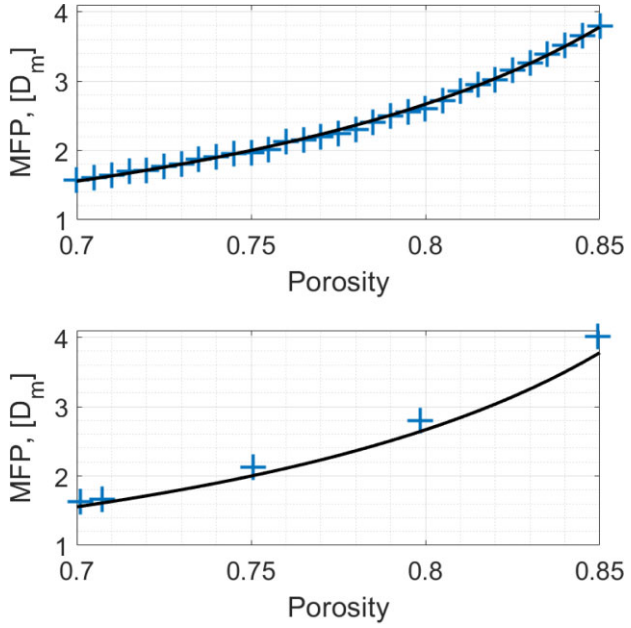

Figure 2. MFP is shown as a function of layer porosity for uniform layers. Results are displayed for hierarchical layers (upper panel) and layers built out of monomers (lower panel). Computational results (crosses) and theoretical curves are shown. Different implementations of building a BAM2 aggregate and various numbers of monomers in an aggregate (from 128 to 512) were used for hierarchical layers.

distribution of the emitted molecules. It was observed that angular collimation along with gas heating takes place, e.g. the angular distribution of the velocity vector differed from the semi-Maxwellian one. These results were applied to derive the reactive force arising from ice sublimation. The analysis of Rosetta's observations gave new impetus to the study of the above effects. Keller et al. (2015b) and Mottola et al. (2020) studied the change in the rotation period influenced by the sublimation activity of the irregular shape of the nucleus. Marschall et al. (2019) and Pinzón-Rodríguez et al. (2021) demonstrated that the change of the gas characteristics (number density and velocity distribution function) noticeably affects the interpretation of observations made by the MIRO instrument onboard the orbiter. We will return to the discussion of this influence below.

In this subsection, we present a new model for estimating the depth of the last scattering for various porous random layers of particles and make an approximation for the subsequent estimation of the resulting gas temperature from the corresponding thermal model. To estimate the relative fraction of particles emitted from the layer as a function of depth, the entire layer is divided into sublayers (spatial bins) with a thickness much smaller than the monomer size (usually one-tenth of its size), and the particles released into a coma from the sublayer are counted. The simulation results are presented for homogeneous layers built by monomers and having different porosity (Fig. 3) and for hierarchical layers constructed by porous aggregates of different sizes (Fig. 4). For all examined cases of homogeneous layers of monomers, the relative fraction of emitted particles first increases as we approach the upper part of a layer, and then decreases near the upper boundary. This relative drop appears to be because the distribution of collision points over a surface that scatters particles becomes more and more asymmetric (upper/lower hemispheres) near the top edge of a model layer. (In all models under consideration, the molecules that have left the layer

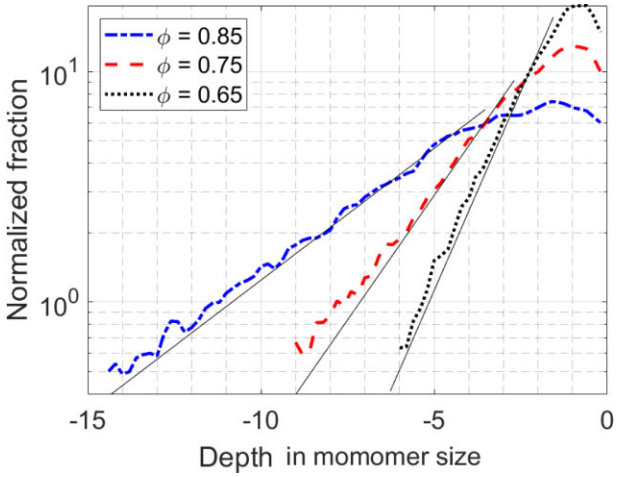

Figure 3. The fraction of particles (in per cent) leaving the layer as a function of depth (a distance from the upper layer boundary) is shown for homogeneous layers of different porosity and constructed by monomers of the same size. Scattered data for small spacial bins and exponential approximation are shown by broken and solid lines, respectively.

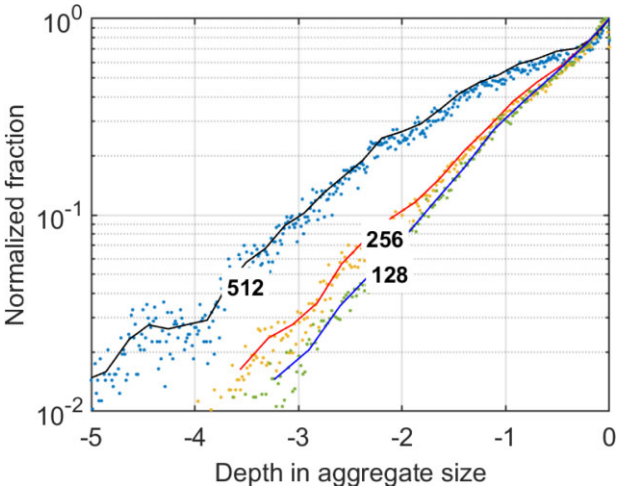

Figure 4. The fraction of particles leaving the layer as a function of depth (distance from the upper layer boundary) is shown for hierarchical layers constructed by aggregates of different sizes. A number on the curve indicates the number of monomers in the aggregate. Scattered data obtained for small spacial bins and moving averages are shown by points and lines, respectively. Typical values of the effective porosity of hierarchical layers are given in Table 1. See details in the text.

do not experience any more collisions, that is, there is no backward flux at all. It is a consequence of the model design which will be rebuilt in future models). The decline observed near the surface is less pronounced for layers of higher porosity. This is consistent with the assumption about the importance of asymmetry mentioned above.

For hierarchical layers, we used various implementations for the aggregate having the selected number of monomers. This approach was used earlier by Skorov et al. (2022). Such aggregates having the same mass slightly differ in general shape, which is manifested in small variations in the distribution of local porosity. The statistical spread of the results is shown in Fig. 4, which also shows the averaged curves for variants of the layers with a fixed mass of the aggregate (i.e. a given number of monomers). For each number of monomers in

the aggregate, we used data for all available 16 implementations of the BAM2 aggregate structure (Shen, Draine & Johnson 2008), each of which is characterized by its specific average porosity. Statistical variations in the internal structure of aggregates explain the observed scattering. Using a fine space step when subdividing a layer to count collisions results in statistical changes in local porosity. Averaging over various statistical implementations of the aggregates and using a coarser spatial decomposition in collision counting allows the smoothing of the averaged curves used to find the approximation coefficients. Since the layers of aggregates have high porosity, the drop near the surface is weakly pronounced (as was the case for the most porous layers of monomers).

It should be remembered that a model assumption about a zero return molecular flux from a coma is an idealization. As is known, during evaporation into a vacuum from an infinite plane, a non-equilibrium Knudsen layer is formed (Kogan & Makashev 1974; Bird 1976). Dozens of articles are devoted to its research, for example, in the application to the physics of comets, the Knudsen layer was studied in (Skorov & Rickman 1998; Skorov et al. 1999; Davidsson 2008). Depending on the type of gas, the relative weight of the back-flow is about 18–25 per cent (Cercignani 1981). These molecules can penetrate the porous layer and collide with the solid phase and be reflected outside, thereby changing the distribution of the depth of the last collision and hence an effective gas temperature. In this study, we do not consider the effect of the Knudsen layer, but it must be studied later. At a qualitative level, it is clear that taking into account the back-flow from the coma will reduce the flattening of the curves near the surface, making the exponential approximation used even more acceptable.

An exponential approximation is satisfactory for the increasing part of the distribution function in all considered cases of homogeneous layers. The corresponding results are shown by solid lines (Fig. 3). Using the exponential form of the approximation, one can speak of the 'effective escape depth'. The estimates of the characteristic depth for homogeneous layers obtained for the approximating exponential function are shown in Fig. 5. The top panel shows the results for hierarchical layers of aggregates of different sizes (N = 128, 256, 512). The bottom panel shows the results for homogeneous layers of spheres. As expected, this characteristic increases with increasing effective porosity or equivalently with increasing MFP. A direct comparison of results for hierarchical and homogeneous monodisperse layers with similar values of effective porosity shows that in layers of aggregates, the effective depth of escape is about twice as big. This effect is evidently because, in the hierarchical layers, there are voids between the aggregates, whose size is noticeably larger than the size of the monomer. The presence of such voids near the upper boundary of the layer significantly increases the chances of particles flying out of the layer. Before proceeding to the analysis of inhomogeneous layers, we note that the random layer structure and the diffuse scattering effectively mix the angular distribution of emitted molecules. No significant deviation from the semi-Maxwellian distribution is observed either for uniform monomer layers or hierarchical layers of aggregates. This result, for all its simplicity, is important for the kinetic modelling of the internal coma by the kinetic methods (e.g. the direct simulation Monte Carlo (DSMC) method).

The effect of an increase in the size of voids observed for hierarchical layers becomes well-pronounced when considering layers with caves. The results of calculations for these layers of different porosity are shown in Fig. 6. Recall that in the model the cavity radius is equal to ten monomer radii (and this is noticeably larger than the size of voids between the largest of the considered

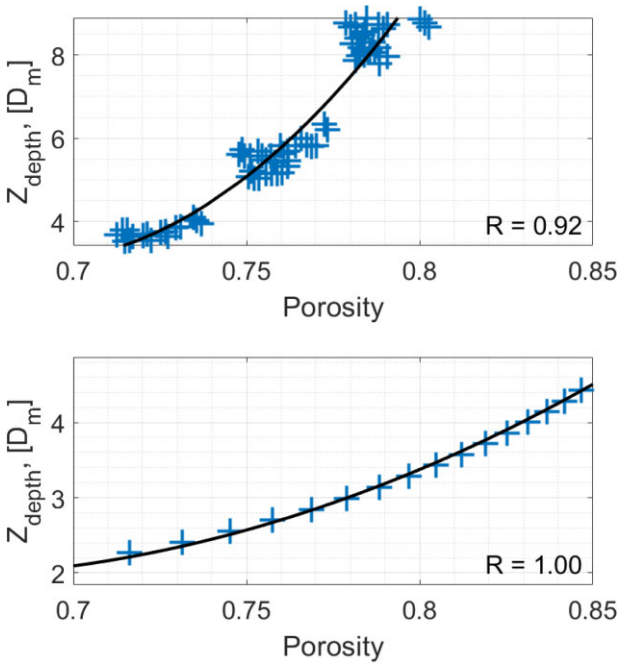

Figure 5. The characteristic depth of the last scattering is presented as a function of porosity for the homogeneous layers. The results are shown for the hierarchical layers (upper panel) and layers built out of monomers (bottom panel). For the layers from aggregates, we used the different implementations of the BAM2 aggregates. This leads to the formation of 'lumps' in the porosity values of the layer. The exponential function was applied for the approximation in both cases.

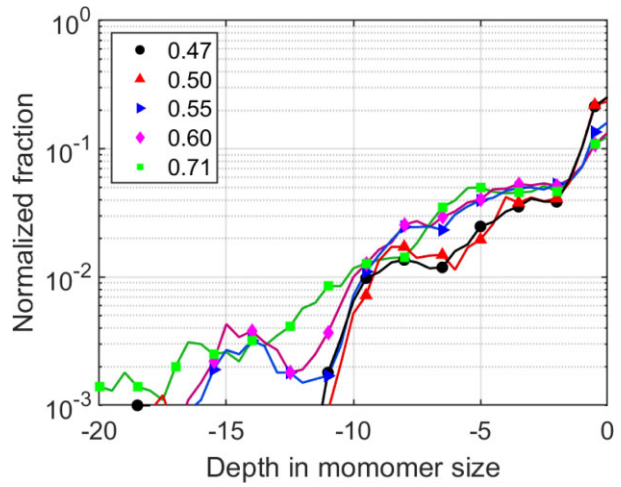

Figure 6. The relative fraction of particles leaving the layer as a function of depth (i.e. a distance from the upper layer boundary). The results are shown for layers of different porosity (see legend). Layers are originally constructed by monomers of two distinct sizes. Caves are obtained by removing the big monomers and have a volume of thousand volumes of small monomers. Moving averages are shown by lines.

aggregates). In the cases under consideration, the presence and relative abundance of cavities near the upper layer boundary can qualitatively change the distribution of the depth at which the last collision occurs. We detect a visible deviation from the smooth behaviour observed for homogeneous layers (see Figs 3 and 4), a doubling of particles ejected from the upper sublayer of about five monomer sizes, and the presence of a 'wavy' behaviour in the

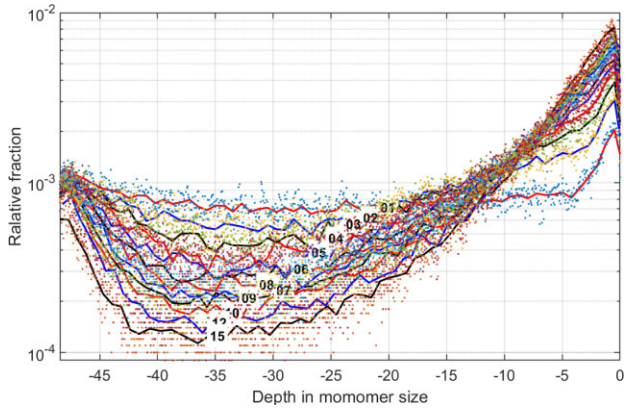

Figure 7. The relative fraction of particles leaving the layer as a function of depth. The results are shown for inhomogeneous layers originally constructed by monomers of one size. Layers have a different number of rectangular slits. The slit width varies depending on their number so that the effective porosity is constant and equal to 85 per cent. Scattered data for small spacial bins and moving averages are shown by points and lines, respectively.

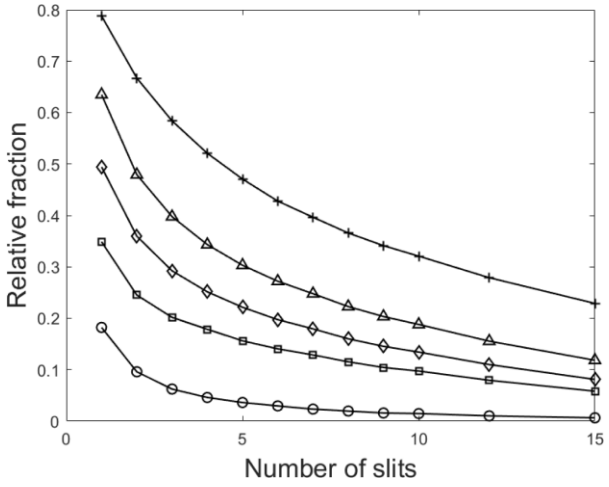

Figure 8. The relative fraction of particles passing through the layer without collision as a function of slit number (or the same, slit width). The dimensionless layer thickness is varied and equals 50, 40, 30, 20, and 10 monomer sizes (curves from bottom to top). Effective layer porosity is fixed and equals 85 per cent.

deeper region associated with the existence of large-scale voids. For such layers, it is not possible to construct an acceptable exponential approximation. Modelling is required on a larger scale and for a larger number of layers to obtain statistically smooth results. Such homogenization and statistical averaging are planned for a future study.

Let us now consider layers with slits. This option is of interest because in this case there are also large voids, but their shape is specific. Since we are considering idealized rectangular slits, there is always a non-zero probability that the particle will pass through the layer without collision if the direction of the initial velocity vector was 'sideways' (the velocity vector is aligned with the slit). Such a division of ejected molecules into two fractions (directly from the bottom and scattered by the walls) is common in models of direct capillaries, which indicates an intermediate place of the considered model with rectangular slits. Note that slit layers were constructed by removing about half of the volume originally occupied by the monomers: the filling factor of an initial homogeneous layer is ∼35 per cent, and for a final layer with slits effective filling factor is only ∼15 per cent. Assuming that the tested domain is a cube and there is only one wide slit in the layer, the dimensionless ratio of its height (equal to the layer thickness) to the width is approximately two, i.e. this is rather a wide rectangular hole than a crack. Thus, the aspect ratio of the aperture basis might be substantial. Obviously, the height-to-width ratio extends linearly with the number of slits and the aspect ratio drops down. This explanation is needed to qualitatively understand the presented simulation results. Fig. 7 shows the relative fraction of molecules that experienced the last collision at a certain depth. It is clearly seen that this distribution is qualitatively different from the distributions obtained for homogeneous layers. First of all, we see a much slower general extinction: the relative number of particles emitted from deeper layers is visibly higher. This effect is due to the special geometry of the voids and the 'side' spans. Regardless of the number of slits, the behaviour of the curves near the upper boundary is qualitatively the same and is similar to the behaviour observed for homogeneous layers: we see a characteristic rise and fall in the vicinity of the edge, giving the typical maximum slightly below the surface. At the same time, we see 'subsidence' in the part of particles emitted from the middle regions and an increase in the proportion near the bottom. Keeping our goals in mind and given the small total of all such particles, we may not worry about this effect, but its simple explanation is not obvious.[1]

This behaviour is plausible as the consideration of gas molecules with small angles of incidence shows: First, only an extremely small fraction of molecules that enter a slit will collide with the slit's wall near its middle height when the slit is very thin. Second, the molecules that hit this middle third have a high probability to hit the slit wall again at lower or higher locations before escaping. So it becomes very improbable for molecules to satisfy both conditions (since the two events are practically independent, the corresponding small probabilities have to be multiplied to obtain the probability of passage with a collision near the middle height). More attention should be paid to the direct release of molecules from the bottom. We have calculated such passing for layers with different thicknesses (e.g. with different slit heights) and different numbers of slits (which determines a slit's width if the layer porosity is fixed). As before, the effective layer porosity is the same and is about 85 per cent. The simulation results are shown in Fig. 8. Layer thicknesses vary from 10 to 50 in increments of 10 in monomer size: this corresponds to curves from top to bottom near the surface and vice versa at deep levels (below about 15 grain diameters). It can be seen that for a layer $10d_s$ thick, even in the case of 15 slits, about 30 per cent of all emitted particles had no collisions, i.e. they emitted directly from the bottom. For a layer $40d_s$ thick, there are slightly less than 10 per cent of such particles. As the slits become wider (at a fixed layer porosity), this proportion always increases somewhat. Our basic task is to estimate the temperature and the distribution function of the velocity of the escaping molecules. Molecules emitted from the bottom retain a temperature equal to the temperature of the subliming

[1]This behaviour is plausible as the consideration of gas molecules with small angles of incidence shows: First, only an extremely small fraction of molecules that enter a slit will collide with the slit's wall near its middle height when the slit is very thin. Second, the molecules that hit this middle and third have a high probability to hit the slit wall again at lower or higher locations before escaping. So it becomes very improbable for molecules to satisfy both conditions (since the two events are practically independent, the corresponding small probabilities have to be multiplied to obtain the probability of passage with a collision near the middle height).

ice and their angular distribution function of the velocity vector is very different from the semi-Maxwellian. It can be concluded that under the idealized assumptions made about the shape of the slits, the role of this fraction is large, and the released gas consists of two components: heated and cold parts. At places without cracks or holes, this effect is of no importance and so not observable.

Summarizing the content of this section, we conclude the following: (i) For all considered cases of homogeneous layers (made of monomers and made of porous aggregates), the depth distribution where the last scattering of test particles occurred is satisfactorily approximated by a simple exponential function. (ii) The characteristic depth grows as expected with an increase in the average chord length or equivalently porosity. (iii) For inhomogeneous layers (both with cavities and slots), a simple exponential approximation does not work well. Layers of such types are poorly amenable to an averaged parametric description and are not considered below.

The presented results show that the effective depth of the last collision in the layer depends on both the porosity and the microstructure of the layer in a non-trivial way. To obtain a simpler estimate of the temperature of the emitted molecules (which would not require complex calculations), one can use as a simplified alternative the general approach proposed by Skorov et al. (1999) and applied in a simplified form in Keller et al. (2015b). This is a model where the porous layer is described as a bundle of straight cylindrical tubes. In this model, all major fluxes can be computed based on simple estimates for probabilities considering isotropic scattering. All the required formulas and discussion can be found in (Skorov et al. 1999). Here, we only give an expression for the resulting probability that a test particle emitted isotropically from a ring of width $d\eta$ and radius r will fly through a horizontal section of the tube located at a distance η from the considered ring. This probability is

$$\mathcal{P}(\eta) = \frac{\eta\,(\eta - \sqrt{4r^2+\eta^2}) + 2r^2}{2\,d\eta\,r\sqrt{4r^2+\eta^2}} \tag{6}$$

To find the number of emitted particles, it is necessary to take into account that the tubes occupy only a part of the control volume and, in the general case, can be randomly oriented. Therefore, the probability of departure must be adapted accordingly for a random porous medium. The capillary model shows dependence on the preliminary pore size but takes into account the pore structure and porosity of the medium in a very simplified way since the simplest dependence of the estimated functions on porosity and tortuosity is assumed. To take into account the 'brokenness' of the tubes and tilt, a tortuosity coefficient τ is usually introduced (see for example the discussion in Skorov et al. 2011), which is associated both with an increase in the average length of the tubes in a layer of thickness L and with an increase in the area of the horizontal cross-section of inclined tubes. These effects are often described in terms of the effective tilt angle of the tube (Epstein 1989). The tortuosity τ lies usually between 1 and 3. In the case of a homogeneous and isotropic distribution of orientations can be expected that $\tau = \sqrt{3}$.

Knowing the fraction of molecules escaping from a ring lying at a certain depth, one can now estimate the 'effective depth' of escaping. To do this, it is necessary to estimate the number of molecules that have experienced a collision in the considered ring. Since it is assumed that the scattering is isotropic, the total number of particles scattered in the ring and having a positive vertical velocity component is simply half of the difference in permeability at the upper and lower lids of the ring multiplied by the starting number of particles. Finally, using the known temperature distribution in the layer, one can calculate the average gas temperature. This idealized model does not replace the computer model presented above but allows one to obtain estimates for cases where information about the layer structure is very scarce. This model also makes it possible to obtain simple analytical estimates for the outgoing gas temperature as a function of the layer thickness, its porosity, and tortuosity.

At first glance, reverting to the Clausing formula may seem unnecessary in light of our more intricate and precise analysis of the flow of gas in a random porous medium. However, its simplicity and utility cannot be overlooked. To understand the role of this idealized description, one must examine the problem of studying comet gas production from a broader perspective. As we noted above, in nearly all thermophysical models investigating energy and mass transfer in the cometary surface layer, the term describing gas production is defined using either the Knudsen or Clausing formula. Despite their inherent drawbacks, these formulas' ability to account for non-isothermal media and even media with volumetric sublimation largely compensates for their limitations. This allows us to progress and employ the modified Clausing formula to model unsteady heat and mass transfer processes (e.g. Davidsson & Skorov 2004). It is on this foundation that we can effectively link the results previously obtained for the structural characteristics of porous media with non-stationary thermal models that account for factors such as gas thermal conductivity and gas heating in a non-isothermal layer. These models will be discussed in forthcoming publications.

4 THERMOPYSICAL CHARACTERISTICS

In continuation of the previous section, here we focus on the quantitative estimation of the characteristics that directly affect the properties of the gas released via Knudsen diffusion through the porous dust layer. These characteristics are included in the heat equation and thus affect the temperature distribution in the layer. Our attention will be directed mainly to the effects associated with the transfer of radiation in a porous layer. We begin by considering the volumetric absorption of incident solar radiation. We then briefly discuss effective thermal conductivity that has already been analysed in detail (Skorov et al. 2022, 2023a, b).

The two-layer model utilized in this study, originally developed by us (Keller et al. 2015a, b), and conceptually rooted in prior works (Mendis & Brin 1977; Brin & Mendis 1979), warrants some elucidation. This model employs several simplifying assumptions. Primarily, we postulate an abrupt change in the ice content across the two layers: the dry porous field layer is devoid of ice, while a constant concentration is maintained in the icy region beneath the interlayer interface. This assumption, albeit a significant idealization, is commonly adopted in modern thermophysical models of the cometary nucleus (e.g. Hu et al. 2017, 2019). This simplification facilitates the reduction of the problem to a single heat equation, as opposed to a system of equations, thereby streamlining the simulation process. It should be noted that sublimation in a porous medium does not transpire on a plane-concentrated boundary, but rather within an effective volume where evaporation and condensation processes are imbalanced. A comprehensive analysis of this issue can be found in (Davidsson & Skorov 2002, 2004), where we also discuss the constraints associated with the application of the continuum approach.

4.1 Volumetric light absorption

As a result of significant voids in the surface layer solar photons are able to penetrate to a depth that may be significant compared to the thermal skin depth and the effective depth of escape. Therefore,

the heat equation must be modified. The history of this issue in publications related to planetary physics goes back to Matson & Brown (1989) and Urquhart & Jakosky (1996) devoted to the study of energy transfer in icy satellites. A so-called solid-state greenhouse effect will occur if the surface layer is optically thin in the visible and opaque in the thermal infrared. Assuming exponential decay of the radiation source as a function of depth with the characteristic e-folding insolation absorption length, they found a remarkable increase in subsurface temperature and non-monotonicity of its distribution. They also emphasized that the amount of subsurface heating is strongly dependent on the assumed thermal properties of the regolith. This process was first implemented in comet models by Davidsson & Skorov (2002). Summary and illustrative examples can be found in Thomas (2021).

Modelling of volumetric absorption of solar radiation in a porous layer is a task that, from the point of view of the implementation in a frame of geometrical optics, is similar to the ones considered above. To solve it by the TPMC method, a parallel flow of photons falls on the lower face of the modelled cuboid. In contrast to the semi-Maxwellian distribution of test particle velocities used earlier for a Knudsen diffusion simulation, it is assumed that all test particles move in the same direction normal to the cuboid face. After generating the starting particle position, the first intersection of the trajectory with the dust skeleton is estimated. Information is collected about the distribution of depths where the first collision of the incoming particle occurred. Since the medium is considered non-scattering, the photon is absorbed at this location. The test ends here and the simulation of the next photon is started.

As before, we start to analyse various homogeneous layers. Some illustrative results are shown in Fig. 9. On the top panel, the distribution of the depth of the first collision is shown for monodisperse layers of spheres. The porosity is indicated in the plot. The bottom panel shows the results obtained for layers made by porous aggregates of different sizes (i.e. containing a different number of monomers) and constructed with and without contact control between aggregates (for details see Skorov et al. 2022). The types of porous aggregates used are displayed in the figure. The examined model layers have effective porosity lying in the range expected for cometary materials.

For the simulation results, we expected to obtain a satisfactory approximation with the exponential Bouguer–Lambert–Beer attenuation law (Modest & Mazumder 2021). The corresponding exponential approximation curves are shown in the same figure. The approximation coefficients are given in Table 1. As one could predict, the radiation penetrates deeper regions more efficiently with increasing porosity. At typical values of nucleus porosity, the total thickness of the absorbing layer of monomers is about 10 dust particle sizes and approximately 30 per cent of direct solar radiation penetrates to a depth of 3–4 dust particle sizes. Note that the void size plays a crucial role when considering attenuation in the opaque layer. The MFP of our model hierarchical layers is much bigger than it is in the case of layers of monomers. The typical radiation penetration depth in hierarchical layers having comparable values of the effective porosity is 3–4 times larger than for the layers of monomers: about 10 per cent of the direct radiation is preserved at a depth of 15–30 sizes of monomers.

The results obtained from simulations of inhomogeneous layers are similar to those reported at the end of the last section when Knudsen diffusion was considered. For the case of layers with vertical rectangular slits, we obtain a fraction of radiation that can penetrate to arbitrary depths. This is an artefact, a consequence of the idealized form of the slits and does not deserve detailed analysis. In layers

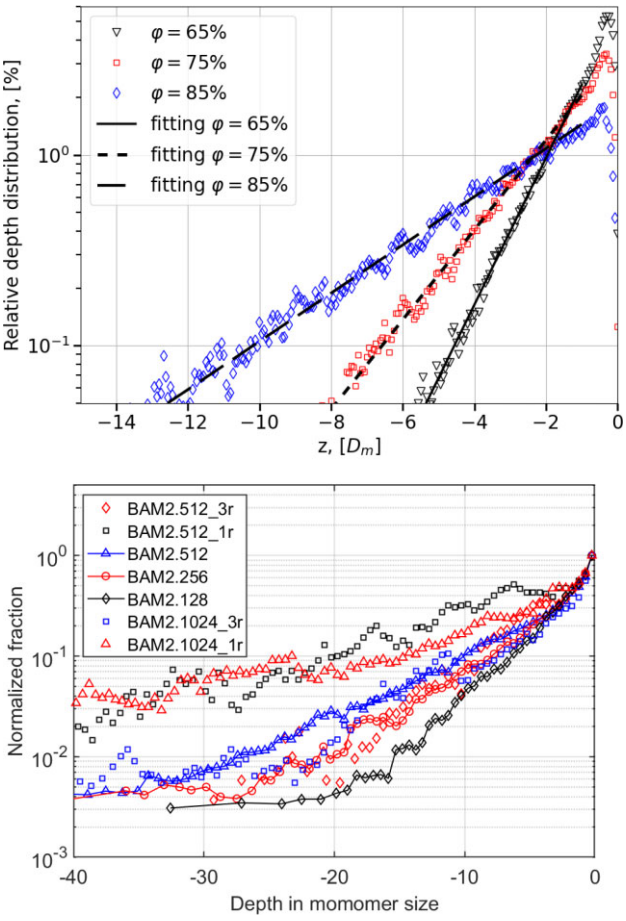

Figure 9. The relative intensity of the normal incident flux of particles as a function of the depth of the first collision expressed in monomer sizes. The results for homogeneous layers of monomers are shown (top panel). The cases of hierarchical layers constructed from ballistic aggregates of different sizes are shown in the bottom panel. Layers designed with and without contact control between the aggregates were tested. The coefficients of the approximation exponential functions constructed for the depths greater than a monomer's diameter are given in Table 1.

Table 1. Coefficient C of approximation exponential function $\exp(-Z/C)$ estimated for hierarchical and monodisperse layers of different porosity.

Layer	Porosity, (per cent)	MFP, (D_m)	C, (D_m)	C/MFP
BAM2.128	73	1.783	3.41	1.912
BAM2.256	77	2.204	4.82	2.187
BAM2.512	80	2.579	6.64	2.575
BAM2.512s-r	85	3.938	9.9	2.514
BAM2.512s-3r	68	1.631	4.4	2.698
BAM2.1204s-3r	76	2.133	5.9	2.766
BAM2.1024s-r	88	4.875	10.1	2.072
Monodisperse	65	1.304	1.13	0.867
Monodisperse	70	1.633	1.45	0.888
Monodisperse	75	2.109	1.85	0.877
Monodisperse	80	2.834	2.44	0.861
Monodisperse	85	4.106	3.44	0.838

with cavities, the effects that we observed in the analysis of the release depths (e.g. the appearance of non-monotonicities, gaps, and secondary peaks) are well manifested again. All these effects are due to sharp changes in the transport properties of the layer on the scale of the cavity size. Such complex layers cannot be properly described by a simple attenuation law. However, as we noted above, these non-homogeneous layers can not be straightforwardly included in one-dimensional heat transfer models, which is the aim of this study. For this reason, and given that the simulations for inhomogeneous and homogeneous media produce qualitatively similar results, we will consider hereafter only homogeneous layers.

The results shown above are obtained in a model where the layer structure is described very accurately, but the radiative transfer is represented in the simplest idealized manner: a geometric optics approximation and perfectly opaque dust are considered. Therefore, of undoubted interest is the comparison of these results with a more sophisticated optical simulation. To this end, we use an approach similar to the one applied in Skorov et al. (2023b) to estimate the radiative thermal conductivity of the porous layer.

To model solar light absorption in a layer consisting of BAM2 aggregates with 256 spheres, the radiative transfer (RT) equation is solved in which the input parameters are the ensemble-averaged scattering properties of individual aggregates corrected by the static structure factor as described by (Ito, Mishchenko & Glotch 2018). First, we use the fast superposition T-matrix method (FaSTMM; Markkanen & Yuffa 2017) to compute the ensemble-averaged scattering phase function and the scattering and absorption cross-sections for the aggregates. The monomer radius was 0.5 microns and the refractive index was $1.6 + i0.1$, corresponding to organic refractory material. Computations were carried out for the wavelength range 0.2–3.0 microns covering most of the incoming solar radiation energy. Second, we apply the static structure factor correction to account for the correlated positions of the aggregates in the layer. The aggregates were assumed to be solid spheres with an effective radius $R_{\rm eff}$ (equals $\sqrt{5/3} * R_{\rm G}$, where $R_{\rm G}$ is a radius of gyration) to use the Percus–Yevick approximation for the pair distribution function (Wertheim 1963). The static structure factor depends on the effective radius, wavelength, and porosity. The static structure factor was then used to correct the pre-computed scattering matrices of the BAM2 aggregates and to calculate the mean free path-lengths and the single scattering albedos for each wavelength that are the input parameters for the radiative transfer solver. Finally, the 1D RT equation was solved using the pre-computed input parameters for each wavelength. The absorption coefficient was extracted from the solution by fitting the exponential function to the absorbed power distribution. For a homogeneous layer of monomers, the same approach was used except the scattering properties of the aggregates computed by FaSTMM were replaced by the Mie solution for spherical particles.

For layers of monomers (Fig. 10 top panel), the simplest idealized model using the TPMC method shows satisfactory agreement with the results of much more sophisticated radiative transport simulations. For layers with high porosity, the agreement is good, but in the worst case when the layer porosity is about 65 per cent, the difference between models is about 50 per cent. For our study, this result is still satisfactory. When comparing the results for layers of aggregates, it should be taken into account that in the model based on RT theory, the effective layer porosity was somewhat higher than in the model using the test particle method. This is due to the way the layer was described in the first case (see the description above). For the TPMC case, only for the case of loose layers built without contact control, the values of effective porosity overlap allowing a direct comparison. Nevertheless, the overall picture looks encouraging:

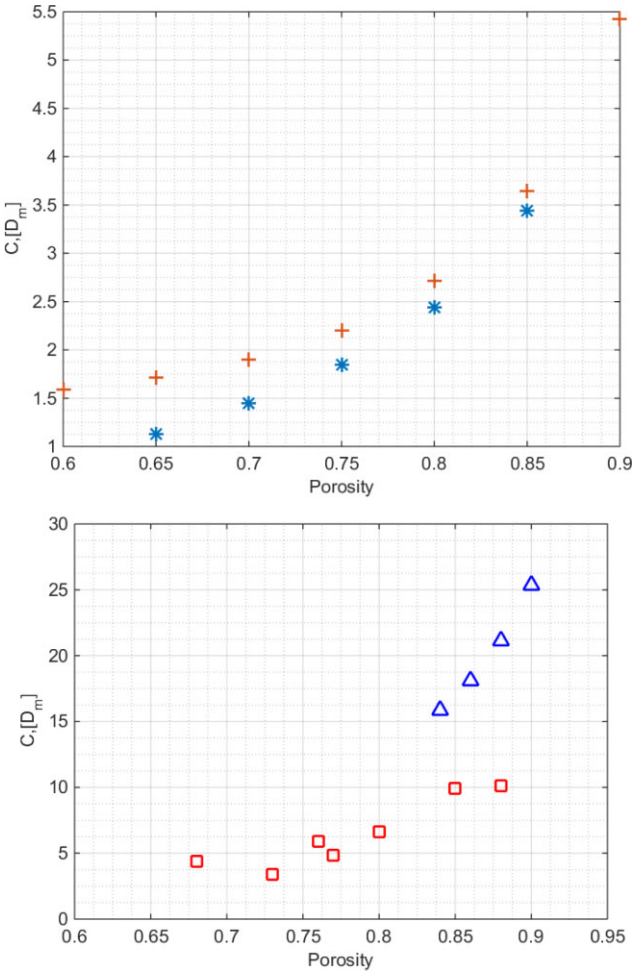

Figure 10. Comparison of direct sunlight attenuation coefficient of approximation exponential functions. The results are presented for homogeneous layers of monomers (upper panel: asterisks and crosses for a test particle model and an RT model, respectively) and aggregates (lower panel: squares and triangles for a test particle model and an RT model, respectively).

where the porosities are close, the results are comparable. Finally, we note that the difference between the models also lies in the fact that there is a small amount of scattering in the RT model, i.e. the particles are not absolutely opaque. This specific feature also leads to some increase in penetration (what one can see in the plot).

We use the obtained attenuation coefficient estimates in thermal models by adding an energy source function that varies with depth (as it was suggested by Davidsson & Skorov 2002; Thomas 2021). Obviously, the addition of a volumetric energy source violates the basic feature of *Model B* about the monotonic behaviour of temperature in the surface layer. In this case, it is necessary to solve the classical non-linear transient heat equation. Using the model from (Skorov et al. 2016), we performed illustrative calculations for a 1 cm thick layer containing millimetre-sized aggregates. As an example, we used one point on the surface of Comet 67P receiving a maximum illumination of about 300 $\mathrm{W\,m^{-2}}$. Fig. 11 shows the temperature distribution on the surface, at a depth of 5 mm, and at the ice sublimation front (1 cm). It also shows how the temperature changes with depth during one rotation period: the curves are plotted with one-hour spacing (bottom panel). The effects are clearly visible due to both volumetric absorption of energy (depth of about 3–5 mm) and sublimation of ice (boundary at a depth of 1 cm). The used model

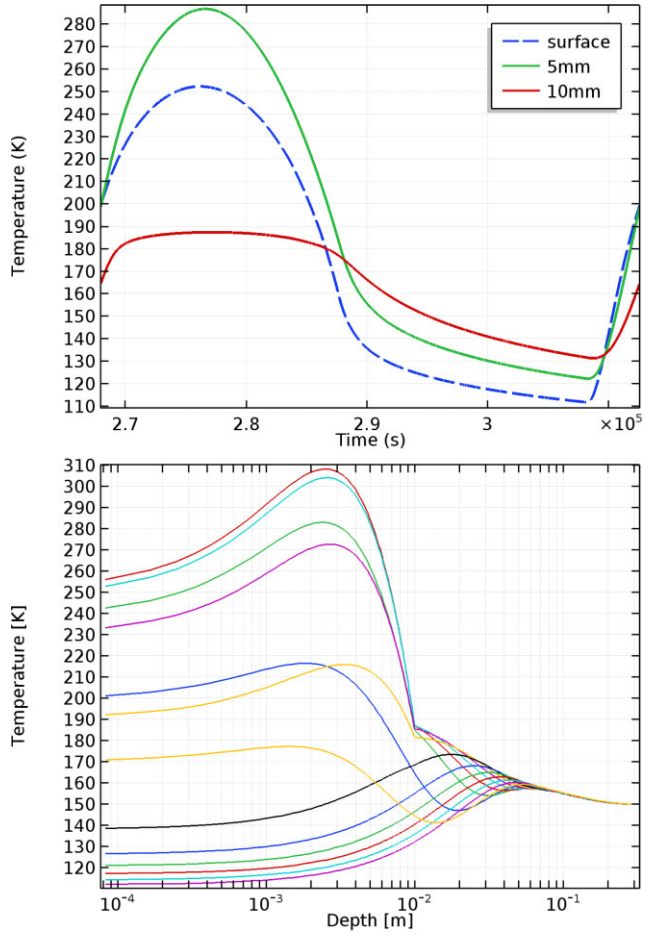

Figure 11. Temperature evolution/distribution in the comet surface layer. The results are obtained for a non-linear non-stationary heat model that takes into account the volume absorption of energy in a porous layer beneath a test point on the surface of a rotating nucleus. The material porosity is 0.75, the aggregate size is 1 mm, and the thickness of the dust layer is 1 cm. The top panel shows the change in temperature on the surface, at a depth of 5 mm, and the sublimation front. The bottom panel shows the change in temperature as a function of depth for one period of comet rotation. The curves are plotted in increments of one hour.

is much more computationally complicated than *Model B* and will not be used in this paper for the general evaluation of the gas heating for a real nucleus shape (see Section 5). The given example shows well that the regions where the volumetric absorption and emission of particles from the layer take place have comparable sizes. Therefore, the extension of (*Model B*) to such a scenario should be considered an urgent task for future research.

4.2 Thermal conductivity

To estimate the kinetic characteristics of the released gas, it is required to obtain the temperature distribution in the non-volatile surface layer by solving the heat equation. That it is necessary to determine all constants of the thermal model as well as the functions included. The latter includes an effective thermal conductivity containing, for typical cometary conditions, the solid phase, and radiative conductivities. We considered these heat transport mechanisms as applied to the surface cometary porous dust layer in detail, for example, in (Skorov et al. 2023b). Below we present a brief review of these mechanisms.

4.2.1 Solid conductivity

The analysis of the solid thermal conductivity of a porous medium, including the case of a hierarchical layer structure, can be found in (Gundlach & Blum 2012). The authors sequentially consider the entire scheme: starting from bulk heat conduction they pass to contact heat conduction between monomers and finally come to heat conduction between porous aggregates. The contact heat conduction between the spheres is studied on the basis of the Hertzian theory of contact t (Kaviany 2012) and the so-called unit-cell approach (Chan & Tien 1973) which makes it possible to proceed to the assessment of the heat conduction of a layer with a regular packing of spheres of the same size. Using implicitly the idea of a hierarchical layer as a layer of pseudo-monomers (i.e. a layer without control of contacts between aggregates) and the adhesive bonding force, to determine the contact area between the particles, the authors propose a general expression for the contact conductivity of a hierarchical porous layer (see Eqs. 14 and 16 there). We emphasize that in the presented analysis, the resulting contact conductivity decreases as the size of the aggregate increases and, based on the results of their experiments, the authors concluded that the solid conductivity of a hierarchical layer of particles larger than one hundred microns is noticeably lower than 0.001 W (K m)$^{-1}$. This value is an order of magnitude smaller than the values commonly applied in cometary thermal models using the conductivity reduction via the so-called Hertzian factor.

Skorov et al. (2023b) evaluated the currently unavoidable uncertainties in the estimation of solid heat conductivity associated with a lack of knowledge of both the composition and the detailed structure (e.g. packing type) of the surface layer as well as aggregate and monomer sizes. It was shown that taking into account this uncertainty strongly affects the resulting gas production (variations can reach several times for a given layer thickness and porosity). For the sake of space, we will not show below the results for various values of this thermal conductivity. However, in evaluating the temperature of the released gas one has to be aware of this uncertainty.

4.2.2 Radiative conductivity

Although the thermophysical model of the 'ice ball' proposed by Whipple (1950) has lost its relevance, it already included the radiative thermal conductivity. Considering a homogeneous grey medium as a bundle of plane-parallel layers, Whipple derived the basic formula for thermal conductivity including the cube of local temperature T, Bond albedo A_b, and thickness of the model layer L. Later, the radiative mechanism of energy transfer was studied in (Mendis & Brin 1977), where the authors introduced the distance between grains (i.e. the average void size) as the characteristic length in a porous granular medium. This resulted in the basic formula that was used in cometary publications without significant changes for many years. It can be written in general form as

$$K_{\rm rad} = 4\sigma A_{\rm em} T^3 l_{\rm ph}, \tag{7}$$

where σ is Stefan–Boltzmann constant, $A_{\rm em}$ is a so-called exchange factor – a constant depending upon emissivity and the geometric factor, $l_{\rm ph}$ is the mean path-length of photons (which equals the mean chord length or the MFP of a test particle in our notation). This Russell's type formula for the radiative conductivity can be obtained (Russell 1935) treating a radiative transfer as a random walk process and using formally the same approach as was applied for a study of transport characteristics of random porous media. A more detailed discussion of the various approximate approaches used to

estimate the geometrical factor, as well as links to specialized books and reviews, can be found, for example, in Skorov et al. (2023b).

Radiative heat conductivity was included in many thermophysical models of the cometary nucleus (see for example Blum et al. 2017; Arakawa et al. 2017; Sakatani et al. 2017; Arakawa, Takemoto & Nakamoto 2019; Hu et al. 2019). This is caused primarily by observational evidence obtained by the Rosetta mission and results obtained by the instruments Multi-Purpose Sensors for Surface and Subsurface Science (MUPUS) (Bentley et al. 2016; Mannel et al. 2019), Cometary Secondary Ion Mass Analyzer (COSIMA) (Langevin et al. 2016; Merouane et al. 2016), and Grain Impact Analyser and Dust Accumulator (GIADA) (Della Corte et al. 2015; Fulle et al. 2015). If the hypothesis that the surface layer of the nucleus consists of large particles ($\gtrsim$1 mm) is correct, then this transport mechanism may be dominant for typical cometary conditions (Gundlach & Blum 2012). An overview of these arguments is presented in (Blum et al. 2017).

The Rosseland's type formulas commonly used in cometary physics are obtained using a number of simplifications and, rigorously speaking, require verification. Such a quantitative comparison of an accurate computational model based on the DMRT (dense media radiative transfer) theory and several popular approximate formulas (models of Rosseland 1936; Van der Held 1952; Chen & Churchill 1963) was performed in (Skorov et al. 2023b). We have shown that among the analysed idealized models, the best agreement with an accurate numerical solution is a Van der Held's model which was suggested for the case of the optically thick isotropically scattering and absorbing medium in a vacuum. It consists of replacing the radiative transfer integro-differential equations with a single heat diffusion equation including a non-linear diffusion coefficient. In this case, the radiative thermal conductivity is expressed by the formula (Van der Held 1952)

$$K_{\rm rad} = \frac{16 n_{\rm r}^2 \sigma T^3}{3\beta}. \tag{8}$$

where $n_{\rm r}$ is the effective index of refraction, $\beta = \kappa_{\rm sca} + \kappa_{\rm abs}$ is the mean extinction coefficient calculated over the entire wavelength range ($\kappa_{\rm abs}$ is the absorption coefficient, κ_{sca} is the scattering coefficient). Note that even for this model, the calculated gas production for millimetre-sized particles can differ by about a factor of two from the results of an accurate numerical DMRT model. The obtained comparisons give us another important estimate of the expected spread of the model results.

A quantitative comparison of the temperatures and corresponding gas productions obtained in the two-layer model (*Model B*) for large aggregates where radiative thermal conductivity can be expected to play an important role can be found in Skorov et al. 2023b (Figs 4–7). In that work, it was also shown that radiative thermal conductivity can be added to the two-layer *Model B* without increasing its computational complexity. This modified model is used below to calculate the kinetic characteristics of the escaping gas.

5 CHARACTERISTICS OF THE ESCAPING GAS FLOW

In the general case, to calculate the characteristics of the escaping gas flow, it is required to solve the transient heat equation for the irradiated dust layer. When the rate of change in insolation on the surface is less than the typical time for establishing a quasi-equilibrium temperature distribution in the near-surface layer, a simplified approach can be used. If the thermal inertia of the medium is small (which is supported by the MIRO instrument observations),

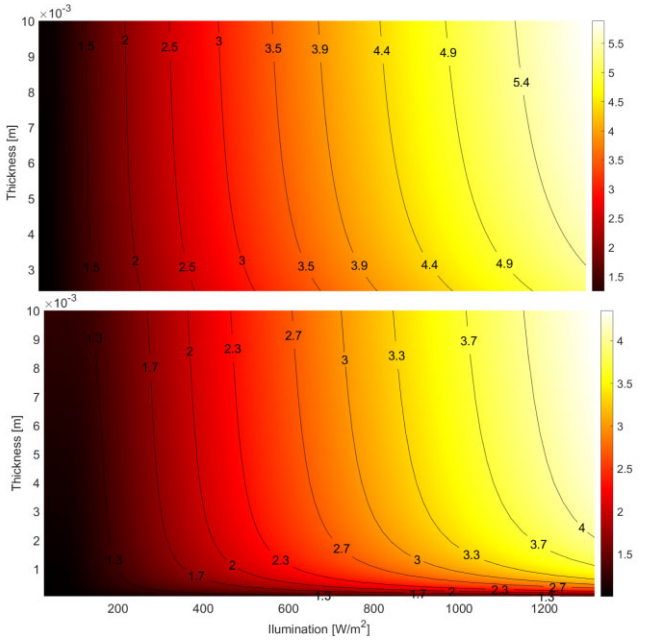

Figure 12. Variation of the radiative thermal conductivity inside a porous hierarchical layer as a function of insolation and layer thickness. The ratio of the value calculated on the surface to the value at the boundary of subliming ice is shown. The size of the aggregates on the upper panel is 1 mm, and on the lower panel – 10 microns. The effective porosity of the layers is approximately 85 per cent.

one can use a model where the solution is found from a system of algebraic non-linear equations that accurately describe the corresponding balance relations for energy flows on the layer boundaries. It was shown in (Skorov et al. 2023b) that this model can be extended to cases where the effective thermal conductivity of the layer includes the temperature-dependent radiative conductivity. Note that, in contrast to the solid conductivity, the radiative conductivities change inside the non-isothermal layer. An illustrative example is shown in Fig. 12 where the ratio of radiative conductivities at the upper and lower boundaries is shown as a function of insolation and layer thickness. On the top panel, the size of the aggregates is 1 mm, on the bottom panel, the size is 10 microns. It can be seen that as the insolation increases, the layer becomes more unevenly heated, and the thermal conductivity changes more strongly with depth. A similar behaviour is observed in the case of small aggregates, although the absolute scatter becomes slightly smaller. Of course, the behaviour of temperature with depth in such models varies non-linearly (which is different from the simplest case of a fixed solid heat conductivity). Therefore, estimates obtained earlier should be revised.

The extended model gives us a practical tool for estimating the required temperatures inside the dust layer. Notice that we have obtained a general solution of the heat transfer equation with the simplifications made. This means that it is possible to obtain an accurate estimate of the temperature of the emitted molecules using all available information about the distribution of temperature with depth. Based on the approximation of the depth distribution of the last collision presented above one can estimate the average gas temperature. An example of such a calculation is shown in Fig. 13. The ratio of the average gas temperature calculated in *Model B* (taking into account the thermal conductivity and non-isothermality of the layer) to the variant when the temperature is simply estimated from the energy balance equation on the surface (model A) is shown.

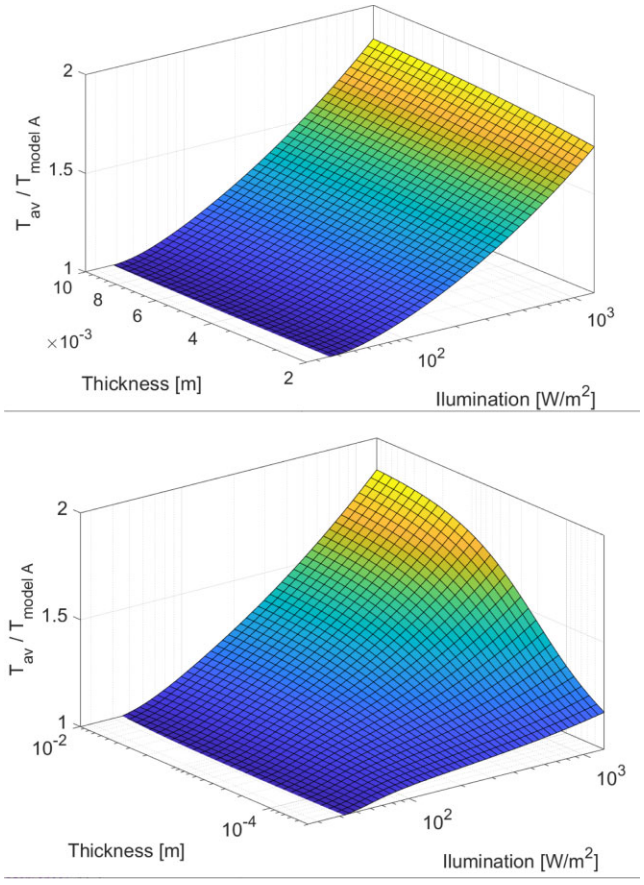

Figure 13. Comparison of the average temperature of escaping gas molecules. The ratio of the value calculated in the two-layer model of a porous hierarchical layer (*Model B*) to the value calculated from the energy budget of the surface (*Model A*) is shown as a function of insolation and layer thickness. The effective porosity of the layers is approximately 85 per cent. The size of the aggregates on the upper panel is 1 mm, and on the lower panel – 10 microns.

In the latter case, it is assumed that the surface has a very low albedo, sublimation is not weakened by the dust layer and the gas is not heated during diffusion. On the top panel, the size of the aggregates is 1 mm, on the bottom panel, the grain size is 10 microns. In both cases, the minimum layer thickness is equal to two aggregate sizes, and the maximum is 1 cm. Effective layer porosity is about 85 per cent. For layers of very large aggregates, the difference increases almost uniformly with increasing insolation, that is, when the radiative thermal conductivity increases rapidly in the same way. For the maximum irradiation level corresponding to a heliocentric distance of about 1 au, the average gas temperature is almost twice as high as the estimate obtained in *Model A*. This result shows how important the considered model modifications are. For the model of small aggregates, the ratio approaches two only when two conditions are met: a high level of insolation and the thickest possible layer. For a given value of irradiation, the surface temperature is higher for thicker layers (which means lower permeability and less sublimation loss). This relative increase in temperature explains the observed increase in the difference in simulation results. It should also be remembered that the effective depth as discussed in Section 3.2 is less than one millimetre in this case. Therefore, the average temperature approaches the very hot surface temperature.

When discussing the temperature of the outflowing gas, the following aspects must be considered. Within the presented model, we investigate the diffuse scattering of molecules upon encountering particles within a non-isothermal dust layer. The model assumes complete energy accommodation during the scattering event. The average temperature discussed below was calculated by summing values across the entire statistical sample of emitted molecules. It is crucial to recognize that the velocity distribution of emitted molecules deviates from the kinetic equilibrium Maxwellian (for which one can only talk about a unified unitary gas temperature). The distribution of emitted molecules also differs, albeit to a lesser extent, from the idealized semi-Maxwellian distribution, corresponding to evaporation from a plane maintained at a specified temperature. Consequently, the question of defining the gas temperature is not straightforward. For further discussion and numerical modelling results utilizing the DSMC method, the reader is directed to Skorov & Rickman (1998).

There is a significant disparity within the Knudsen layer between the kinetic temperatures calculated for the stochastic molecular velocity components parallel and perpendicular to the surface boundary. Thus, at the one mean free path above the surface, this ratio is approximately two and tends to converge to a single value, due to molecular collisions. The non-equilibrium region does not have a distinct boundary. However, approximate Maxwellization seems to be achieved, at least within the statistical uncertainty, at a distance of about 10–20 mean free path from the surface. Davidsson (2008) noted that the size of the non-equilibrium region depends on an appropriate number of Monte Carlo test particles and ensuring adequate spatial and temporal resolution in DSMC simulations. Cercignani (2000) pointed out that local thermodynamic equilibrium is achieved to within 90 per cent at a distance of about 20 mean free path from the surface. Therefore, we show the average temperature here for illustration purposes. To apply our results, for example, in kinetically non-equilibrium models of innermost coma based on the DSMC method, detailed information on the complete velocity distribution of emitted molecules is used.

It is necessary to analyse dozens of combinations of model parameters when solving the problem of obtaining estimates or constraints on the values of environmental characteristics. In this case, the execution speed becomes one of the key properties of the model. In Skorov et al. (2023b) we have paid much attention to the advantages and disadvantages of models of type *A* (where the presence of dust on the surface is not taken into account in any physically acceptable way) and *B* (which is a much more realistic description, at least for periodic comets). Though, in estimating the effective gas production, model *A* can still be somehow useful to fit observations by introducing the arbitrary concept of active fraction (i.e. the comet is only active in specific patches on the surface), yet this model is useless for estimating gas heating.

We have already demonstrated that *Model B* is not much more computationally demanding than *Model A* for calculating gas production. This conclusion is completely valid also in the case of gas heating. As before, this model has absolutely the same level of computational complexity and can be used for a realistic shape model in all cases when we are interested in accurate simulation of the innermost coma. To confirm our conclusion, we show the results obtained for a model that takes into account the real shape of the nucleus of comet 67P. The SHAP7 model from (Preusker et al. 2017) decimated to about 12 500 triangular facets was used. The effective incoming energy flux on the surface was calculated including the effects of shading and re-radiation (Keller et al. 2015b). The calculations were performed for *Models A* and *B* at perihelion and presented in Fig. 14. For *Model*

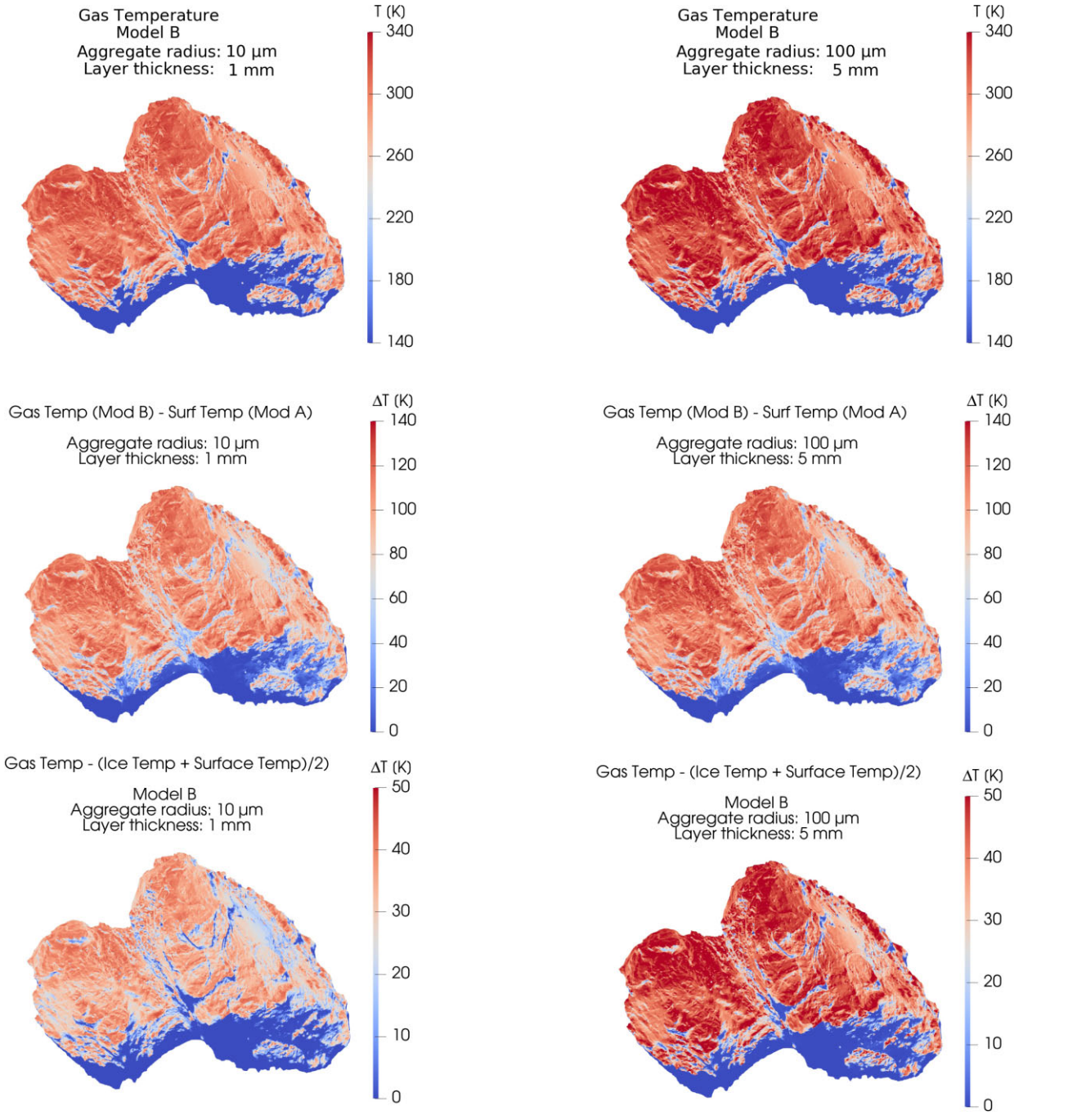

Figure 14. The average temperatures of the gas above the surface of the nucleus of comet 67P at perihelion calculated for various models. The characteristics of the layer in the *Model B* are indicated in the legend. A more detailed description is contained in the text.

B, the radius of porous aggregates was taken to be 10 (left column) and 100 (right column) microns. The thickness of the dust layer was 1 and 5 mm, respectively. Radiative and solid conductivities were included. The permeability depending on the layer thickness and size of the aggregate was also taken into account. The top row shows the average temperature of the emitted molecules in *Models B*. The middle row shows the difference between the calculated temperatures for models *B* and *A*. Finally, the lower row shows the difference in temperatures calculated for *Model B*, which carefully takes into account the distribution of the probability of escape of molecules via the TPMC method, and the case, where the average temperature is simply a half-sum of the temperatures of the nucleus surface and the ice underlying the layer. The latter case illustrates the importance of carefully modelling diffusion in a layer.

A comparison of the results shown in the top row shows that the relationship between the average gas temperature and the properties of the layer is not trivial. Indeed, for a layer consisting of smaller aggregates, the expected value of radiative conductivity is approximately an order of magnitude lower, since this characteristic is directly proportional to the particle size. This could promise a higher temperature of the near-surface layer (and, hence, of the ejected molecules). However, dimensional layer thickness matters because

the heat transfer model does not scale like the Knudsen diffusion model, where only relative characteristics are used. Therefore, a layer 5 mm thick is the best insulator and the gas temperature is slightly higher in this variant.

This relative excess is significantly less than the difference between the results of models *B* and *A* shown in the middle row. This was to be expected since additional heating due to thermal accommodation during the collision of molecules with hot dust particles is completely absent in this case. It is seen that this gas heating is the greater, the higher the insolation. For cold regions, the difference approaches zero, but this similarity of results is irrelevant, as it merely reflects the fact that sublimation becomes extremely weak. It is important to understand that the gas not only becomes colder but also its density drops by many orders of magnitude. This statement can be illustrated by the following example. At the maximum value of insolation for large particles (100 microns), with an increase in the layer thickness from 0.4 to 6 mm, the gas production decreases only by a factor of approximately 7. This is explained by the relative increase in the temperature of the ice underlying the thicker layer (from 214 to 218 K), which partially compensates for the decreased permeability of the layer. With insolation about ten times less, the temperature difference between the thick and thin layers remains about the same ($\sim$3 K), but the temperature itself decreases by about 20 K. Due to the exponential dependence of gas production on temperature, this decrease leads to a decrease in gas density by about 25 times. In this case, the difference in the average gas temperatures estimated in different models decreases to about 10 per cent.

Finally, let's look at the results shown in the bottom row of the figure. Here, we show a comparison of the average temperatures calculated in *Models B* with and without taking into account the non-linear form for the distribution of the depth of the last collision of a molecule with a porous skeleton. As discussed above, several approximations can be used to estimate this distribution. The most accurate one can be obtained from the model of a porous layer consisting of individual particles by the TPMC method (as done above). As an intermediate approximation having a fully analytical form, the model of cylindrical capillaries can be used. In this model, the depth distribution for the last collision remains a non-linear function, but the dependence on porosity and tortuosity is taken into account in the simplest form. Finally, it can be assumed that the molecules fly out with the same probability, independent of depth and there is a linear T-decrease with depth (a case without a volume energy absorption). Then, the average gas temperature is simply half the sum of the surface temperature and the temperature of the subliming ice. Note that only this approximation is available if the Knudsen diffusion model and layer microstructure are not used. The comparison results show that the latter approximation is very coarse, although it remains preferable to using *Model A*. The temperature difference is several tens of Kelvin for well-illuminated areas of the nucleus. Since it is these regions that make the main contribution to gas productivity, the use of such an approximation for the analysis of observations is undesirable.

6 CONCLUSION

Obtaining estimates for the temperature of the gas at the boundary of the surface of the comet nucleus is an acute problem in cometary physics. For many years this problem has attracted attention because the temperature of a gas determines its velocity. The macroscopic flow velocity, in turn, is important for estimating non-gravitational perturbations in the motion of a comet due to the resulting recoil force. In addition, gas velocity is important in assessing the acceleration of the inert dust fraction in a coma, which determines the observed structures of the scattering dust coma.

Added to these classic problems are new ones related to the analysis of unique observations obtained by the Rosetta spacecraft. For the first time, we were able to directly analyse the characteristics of the gas in the inner coma near the nucleus. The analysis already performed has shown that the gas is significantly hotter (and faster) than the simplest estimates from the energy balance for ice on the surface give (Marschall et al. 2019; Pinzón-Rodríguez et al. 2021; Rezac et al. 2021). This effect is undoubtedly related to the interaction between the gas and the hot porous layer of dust covering the surface.

In this paper, we have carried out a thorough analysis of Knudsen diffusion through non-isothermal porous layers. All the variety of model layers analysed in recent articles (Skorov et al. 2021, 2022, 2023a, b) was considered. Homogeneous random layers made of solid particles (mono- and bi-modal) and porous aggregates as well as inhomogeneous layers with cavities and cracks were considered. It was assumed that the collision of molecules with a solid phase takes place with complete energy accommodation. To estimate the distribution of the depth of the last collision (which determines the distribution of the velocities of the emitted molecules), the Test Particle Monte Carlo method was used. Based on the obtained numerical simulation results, approximating functions were obtained and used together with the solution for the temperature distribution in the layer obtained in the two-layer heat transfer model. This model takes into account the resistance of the porous layer to gas flow and the effective thermal conductivity, which is a function of temperature.

It was shown that molecules can escape from a wide depth range of a layer whose thickness depends on the porosity of the layer and the size of the voids, which in turn is related to the characteristic size of the particles. Since the solution to the problem of heat distribution in a layer is not scalable like the problem of Knudsen diffusion, where only relative dimensionless quantities are used, the calculation of the average gas temperature requires the use of a thermal model for layers of different structures. The modelling performed showed that the average temperature is sensitive to all the main parameters of the model (i.e. porosity, particle size, layer thickness). The use of the general approach suggested in (Skorov et al. 2023b) to calculate the gas productivity, taking into account the effective illumination and the complex shape of the nucleus (in the example of comet 67P) made it possible to create an effective model that can be directly used in complex computational models of the internal kinetically non-equilibrium coma (Marschall et al. 2019). We have shown that simpler models used to estimate the average temperature lead to significant errors. These differences are the more significant the higher the level of insolation and hence the intensity of sublimation. The proposed scheme does not lead to any noticeable additional computational costs and can be recommended for further use. The next step of our research will be connected precisely with the modelling of non-equilibrium coma and the analysis of observations made by the MIRO instrument (Pinzón-Rodríguez et al. 2021).

The porous structure of the surface layer implies that not only molecules can fly out of a certain volume, bearing an imprint of the temperature distribution in this region, but sunlight is absorbed not only on the surface. Radiation effectively penetrates into deeper layers, which radically changes the energy balance and temperature profile there. In cometary publications, this effect came into focus about twenty years ago. It has been confirmed in laboratory experiments and has so far been associated mainly with gas production estimates. For the first time, we have shown by examples that the regions of absorption of solar radiation and the effective emission of molecules are comparable in size. Volumetric energy absorption

leads to the fact that the temperature profile in this region becomes essentially non-monotonic and the maximum is reached at some depth and not at the surface. All these effects were proven to be extremely sensitive not only to the effective porosity but also to the actual size of the aggregates and the eventual presence of non-homogeneities like cracks and cavities. Preliminary calculations showed that more research is needed here and *Model B* should be extended and adapted to this process. This problem will be considered in our upcoming study.

ACKNOWLEDGEMENTS

YS acknowledges support from ESA through contract 4000141229/23/ES/CM and the Deutsche Forschungsgemeinschaft (DFG) for support under grant BL 298/32-1. We also thank the International Space Science Institute, Bern, Switzerland for providing support and a facility for collaboration.

DATA AVAILABILITY

The data underlying this article will be shared on reasonable request to the corresponding author.

REFERENCES

Arakawa S., Tanaka H., Kataoka A., Nakamoto T., 2017, A&A, 608, L7
Arakawa S., Takemoto M., Nakamoto T., 2019, Prog. Theor. Exp. Phys., 2019, 093E02
Asaeda M., Yoneda S., Toei R., 1974, J. Chem. Eng. Japan, 7, 93
Bentley M. S. et al., 2016, Nature, 537, 73
Bird G. A., 1976, NASA STI/Recon Technical Report A, 76, 40225
Blum J. et al., 2017, MNRAS, 469, S755
Brin G. D., Mendis D. A., 1979, ApJ, 229, 402
Cercignani C., 1981, Prog. Astronaut. Aeronaut., 74, 305
Cercignani C., 2000, Rarefied Gas Dynamics. Cambridge Univ. Press, Cambridge, UK, p. 338
Chan C. K., Tien C. L., 1973, Trans. ASME, J. Heat Transfer, 95, 302
Chen J. C., Churchill S. W., 1963, AIChE J., 9, 35
Clausing P., 1932, Ann. Phys., Lpz., 404, 961
Davidsson B. J. R., 2008, Space Sci. Rev., 138, 207
Davidsson B. J. R., Skorov Y. V., 2002, Icarus, 159, 239
Davidsson B. J. R., Skorov Y. V., 2004, Icarus, 168, 163
Della Corte V. et al., 2015, A&A, 583, A13
Derjaguin B., 1946, Dokl. Akad. Nauk SSSR, 53, 687
Epstein N., 1989, Chem. Eng. Sci., 44, 777
Fulle M. et al., 2015, ApJ, 802, L12
Groussin O. et al., 2019, Space Sci. Rev., 215, 29
Gundlach B., Blum J., 2012, Icarus, 219, 618
Van der Held E., 1952, Appl. Sci. Res., Section A, 3, 237
Hu X. et al., 2017, MNRAS, 469, S295
Hu X., Gundlach B., von Borstel I., Blum J., Shi X., 2019, A&A, 630, A5
Ito G., Mishchenko M. I., Glotch T. D., 2018, J. Geophys. Res. Planets, 123, 1203
Kaufmann E., Kömle N. I., Kargl G., 2006, Icarus, 185, 274
Kaviany M., 2012, Principles of Heat Transfer in Porous Media. Springer-Verlag, Berlin
Keller H. U. et al., 1986, Nature, 321, 320
Keller H. U., Delamere W. A., Reitsema H. J., Huebner W. F., Schmidt H. U., 1987, A&A, 187, 807
Keller H. U., Mottola S., Skorov Y., Jorda L., 2015a, A&A, 579, L5
Keller H. U. et al., 2015b, A&A, 583, A34
Keller H. U. et al., 2017, MNRAS, 469, S357
Knudsen M., 1909, Ann. Phys., Lpz., 333, 75
Kogan M. N., Makashev N. K., 1974, Fluid Dyn., 6, 913
Langevin Y. et al., 2016, Icarus, 271, 76
Macher W., Skorov Y., Kargl G., Laddha S., Zivithal S., 2023, J. Eng. Math., 144
Mannel T. et al., 2019, A&A, 630, A26
Markkanen J., Yuffa A. J., 2017, J. Quant. Spectrosc. Radiat. Transfer, 189, 181
Marschall R. et al., 2016, A&A, 589, A90
Marschall R. et al., 2019, Icarus, 328, 104
Matson D. L., Brown R. H., 1989, Icarus, 77, 67
Maxwell J.C., 1879, Phil. Trans. R. Soc., 170, 231
Mendis D. A., Brin G. D., 1977, Moon, 17, 359
Merouane S. et al., 2016, A&A, 596, A87
Modest M., Mazumder S., 2021, Radiative Heat Transfer. Elsevier Science, New York
Mottola S., Attree N., Jorda L., Keller H. U., Kokotanekova R., Marshall D., Skorov Y. V., 2020, Space Sci. Rev., 216, 2
Pinzón-Rodríguez O., Marschall R., Gerig S. B., Herny C., Wu J. S., Thomas N., 2021, A&A, 655, A20
Preusker F. et al., 2017, A&A, 607, L1
Reshetnik V., Skorov Y., Bentley M., Rezac L., Hartogh P., Blum J., 2022, Sol. Syst. Res., 56, 100
Reshetnyk V., Skorov Y., Vasyuta M., Bentley M., Rezac L., Agarwal J., Blum J., 2021, Sol. Syst. Res., 55, 106
Rezac L. et al., 2021, A&A, 648, A21
Rosseland S., 1936, Theoretical Astrophysics. The Clarendon Press, Oxford
Russell H., 1935, J. Am. Ceram. Soc., 18, 1
Sakatani N., Ogawa K., Iijima Y., Arakawa M., Honda R., Tanaka S., 2017, in 48th Annual Lunar and Planetary Science Conference No. 1964. LPSC Press, Houston, Texas, US
Schloerb F. P. et al., 2015, A&A, 583, A29
Shen Y., Draine B. T., Johnson E. T., 2008, ApJ, 689, 260
Skorov Y., Rickman H., 1995, Planet. Space Sci., 43, 1587
Skorov Y. V., Rickman H., 1998, Planet. Space Sci., 46, 975
Skorov Y. V., Kömle N. I., Markiewicz W. J., Keller H. U., 1999, Icarus, 140, 173
Skorov Y. V., Keller H. U., Rodin A. V., 2008, Planet. Space Sci., 56, 660
Skorov Y. V., Keller H. U., Rodin A. V., 2010, Planet. Space Sci., 58, 1802
Skorov Y. V., van Lieshout R., Blum J., Keller H. U., 2011, Icarus, 212, 867
Skorov Y. K., Rezac L., Hartogh P., Bazilevsky A. T., Keller H. U., 2016, A&A, 999
Skorov Y. V., Rezac L., Hartogh P., Keller H. U., 2017, A&A, 600, A142
Skorov Y., Reshetnyk V., Rezac L., Zhao Y., Marschall R., Blum J., Hartogh P., 2018, MNRAS, 477, 4896
Skorov Y. V., Keller H. U., Mottola S., Hartogh P., 2020, MNRAS, 494, 3310
Skorov Y., Reshetnyk V., Bentley M., Rezac L., Agarwal J., Blum J., 2021, MNRAS, 501, 2635
Skorov Y., Reshetnyk V., Bentley M. S., Rezac L., Hartogh P., Blum J., 2022, MNRAS, 510, 5520
Skorov Y., Reshetnyk V., Küppers M., Bentley M. S., Besse S., Hartogh P., 2023a, MNRAS, 519, 59
Skorov Y., Markkanen J., Reshetnyk V., Mottola S., Küppers M., Besse S., El-Maarry M. R., Hartogh P., 2023b, MNRAS, 522, 4781
Thomas N., 2021, An Introduction to Comets: Post-Rosetta Perspectives (Astronomy and Astrophysics Library). Springer-Verlag, Berlin
Thomas N., Keller H. U., 1989, A&A, 213, 487
Thomas N., Davidsson B., Jorda L., Kührt E., Marschall R., Snodgrass C., Rodrigo R., 2021, Cometary Science: Insights from 67P/Churyumov-Gerasimenko (Space Sciences Series of ISSI). Springer-Verlag, Berlin
Tsang L., Pan J., Liang D., Li Z., Cline D. W., Tan Y., 2007, IEEE Trans. Geosci. Remote Sens., 45, 990
Urquhart M. L., Jakosky B. M., 1996, J. Geophys. Res., 101, 21169
Wertheim M. S., 1963, Phys. Rev. Lett., 10, 321
Whipple F. L., 1950, ApJ, 111, 375

This paper has been typeset from a TEX/LATEX file prepared by the author.